# Synthesis of α-Al2O3 Nanoparticles From Pepsi Cans Wastes and Its Fungicidal Effect on Some Mycotoxins Producing Fungal Isolates

**Asmaa Ismail**
National Research Centre
**Hoda Kabary**
National Research Centre
**Ahmed Samy** ( asamy1@yahoo.com )
National Research Centre https://orcid.org/0000-0002-7836-2592

**Research Article**

**Keywords:** Isolate mycotoxin producing fungal, α-aluminium nanoparticles, Pepsi cans wastes, Recycling wastes, Antifungal activity

**Posted Date:** August 5th, 2021

**DOI:** https://doi.org/10.21203/rs.3.rs-774484/v1

# Abstract

Green synthesis of nanomaterials is the most recent trend in nanotechology because it is synthesized the highly valuable compounds (nanomaterials) from wastes to reduce the highly negative impact of these wastes in environment. The aim of this study was to isolate and purify the most common mycotoxin, aflatoxin producing fungi from Maize and soybean grains which considered as the great economical importance as both animal and human feed. In addition to green synthesized of a-$Al_2O_3$ from cans and to detect its antifungal effect on the isolate's growth at different concentrations. Thereafter, determining the fungicidal concentration of the tested nanoparticles on the isolated fungal strains. The structural, morphological, optical and antifungal activity of the prepared a-$Al_2O_3$. are characterized using X-ray diffraction (XRD), High resolution transmission electron microscope (HRTEM), Field Emission Scanning Electron Microscope (FESEM), Attenuated total Reflection-Fourier Transform Infrared (ATR-FTIR) and Ultraviolet-Visible (UV-Vis) spectrophotometer. Results shows that, the most common fungal strains presented were belonging to Aspergillus flavus, Fusarium oxysporum and Alternaria sp.. Formation of $Al_2O_3$ is confirmed using XRD, FESEM and ATR –FTIR. The average particle size of a-$Al_2O_3$ is 4-10 nm. Optical band gap of a-$Al_2O_3$ are calculated using Tauc relation. Through investigating the fungicide concentration, Data showed that the maximum antifungal activity of aluminum nanoparticles a-$Al_2O_3$ was detected for A. flavus, Fusarium sp.and Alternaria sp. in concentration 1, 6 and 50 mg/100ml respectively.


# Introduction

In recent years, Scientists have recently turned to green synthesis of nanoparticles from wastes and used these in many applications. The valuable use of nanoparticles is their superior antimicrobial efficacy as compared to their bulk counterparts. There is a growing need to develop new and effective antimicrobial agents as the threat of bacterial and fungal infections grows.

Nanoparticles have also been used in food preservation, burn dressings, medical equipment, water treatment, and a variety of other items in this direction [1, 2].

Wastes come from Aluminum cans makes a great problem in the environment. So, recycling of this type of waste save money, energy and time in addition to the money that comes from recycling cans helps people and their communities [3–5]. Due to its distinct physical and chemical properties, alumina has a wide range of industrial applications.

Aluminum oxide comes in a variety of types, all of which are produced by calcining the aluminum hydrates bayerite, gibbsite, and boehmite [6]. α-$Al_2O_3$ nanopowder is one phases from many type of alumina and it take attention due to it is high chemical resistance, high abrasion resistance and high thermal stability [7]. Due to a favorable combination of properties such as high mechanical strength and hardness, strong wear resistance, high refractoriness, and high corrosion resistance in a wide variety of chemical environments, $Al_2O_3$ is one of the most commonly used ceramic materials [8].

In developing countries, Maize and soybean grains are considered major crops for human and animal feed due to its relatively high protein and suitable amino acid concentration that simultaneously affect the health, breeding and productivity. Inappropriate preservation of Maize and soybean usually causes the yield to be infected till spoilage with saprotrophic, mycotoxin producing fungi unless treated with fungicide during the storge period. Animal feeding on spoiled grains lead to accumulative, detrimental effect generally on the animal health and preciously on productivity [9]. The most common fungal infection included but not limited to: Aspergillus sp., Alternaria sp. and Fusarium sp. [10]. Different types of mycotoxins are produced by different fungi, Aflatoxin production relatively distinct to Aspergillus infection, fumonisin is produced commonly by Fusarium species. Other fumonisin related mycotoxins such as tenuazonic acid, alternariol characteristically distinct to Alternaria infection [11].

The application of synthetic fungicide for long term is not ideal due to its high cost, residues and eventually its impact on the environment and general health. Moreover, the increased resistance of the fungal pathogen towards the fungicide is another setback for the wide and continuous application of chemically synthesized fungicide [12].

Recently, the wide application of nanotechnology for the control of vast majority of plant and human infection against different pathogenic microbes, have attracted increasing attentions as substitute for their chemically synthesized counterparts. Nowadays, Nanotechnology plays a major role in the control of plant infection either through limiting agent transmission or disease detection [13, 14]. Additionally, nanotechnology is becoming a potential solution for food borne pathogen control and elimination. In precious, Aluminum nanoparticles have been used for multiple environmental applications due to its wide- known, potent antimicrobial characteristics as food preservative substance.

In our research work, we aimed to prepare α-$Al_2O_3$ from Pepsi cans and studied their structural, surface morphology and optical using different tools XRD, ATR-FTIR, HRTEM, FESEM and UV-Vis spectroscopy. Then the antifungal activity of the prepared α-$Al_2O_3$ against the isolated fungal species individually to determine the fungicidal concentration that cause the maximum inhibitory effect on the isolated fungal strains growth.

## Method Of Preparation

# 2.1. Preparation of α-$Al_2O_3$ NPs

Synthesis of α-alumina from Pepsi cans, the materials used were aluminum cans (collected from wastes), HCl (6 N), NaOH (24%) and deionized water. Cut the Pepsi cans into small pieces. After that slowly adding of pieces into 6 N HCl to avoid any risks during the dissolving of aluminum, After the complete dissolved of cans, separation of the solution from any other impurities by filtration using Whatman 42 filter paper. Then adding the 24% NaOH dropwise to the solution till the aluminum hydroxide was obtained. Washed the prtecipitate three times using centrifuge at 1500 g/15min for elimination NaCl. ernight and calcinated at 350°C/3h.

## 2.2. Characterization of α-$Al_2O_3$ NPs:

X-ray diffraction (XRD) is performed PANalytical X'Pert Pro target Cu-Kα with secondary monochromator Holland radiation, the tube operating at 45 kV with 0.1540 nm wavelength) over a 2θ range of (5°–80°). High – Resolution Transmission Electron Microscope (HRTEM) was performed by JEM-2100F electron microscope with accelerating voltage of 200 kV. Field Emission Scanning Electron Microscope (FESEM) with EDX detector was performed using SEM Model Quanta 250 FEG. ATR-FTIR spectral data are collected using Vertex 80 Bruker (made in Germany) at room temperature in the range 4000 – 400 $cm^{-1}$. UV/vis. spectral data collected using Jasco V-630 spectrophotometer in the range 200–1000 nm at room temperature.

## 2.3. Fungal species isolation and identification

Maize and soybean grains that show rotting signs were collected for fungal isolation. The first step involving surface sterilization of the grains by selecting 1 gm of each grain type and soaking in 0.5% sodium hypochlorite for 3 minutes, followed by wishing with sterilized, distilled $H_2O$ three times and allowed to air drying under aseptic conditions. subsequently, dried grains were grinded in mortar and suspended in 9ml sterilized distilled $H_2O$ then vortexed till homogeneity. Serial dilutions were made till the 3rd factor, and 1 ml of the 2nd and 3rd dilution were transferred to rosebengal agar petri dishes and incubated at 30$^oC$ for 5 days. After the incubation period, fungal colony developed were transferred to potato dextrose agar dishes and incubated under the same previous conditions.

For fungi identification, the fungal isolates developed on PDA petri dishes were identified via colony morphology, shape, color and medium pigmentation, as well as microscopic examination of the developed spores and mycelium.

## 2.4.Screening of aluminum nanoparticles' antifungal activity

Aluminum nanoparticles solution was prepared in concentration (2mg/3ml $DDH_2O$) and tested for antifungal activity against *Aspergillus flavus, Fusarium oxysporum*and *Alternaria* sp. 7mm fungal disk of each isolate was cut and inoculated in 10ml distilled sterilized $H_2O$ then vortexed vigorously till obtain Fungal spore suspensions of $10^5$-$10^6$. 1ml of the fungal spore suspension was inoculated in sterilized petri dishes, covered with warm PDA sterilized medium, and mixed homogenously then left till solidification. By mean of sterilize tip end, 7mm agar well was made and inoculated with 50ul (33.3 ug/50ul) of the prepared nanoparticles solution. The PDA plates were left in the fridge for 30 minutes to allow the solution diffusion, then incubated at 30c for 5 day. The antifungal activity was detected after the incubation period by measuring the inhibition zone around the well by ruler in mm.

## 2.5. Determination of the fungicidal concentration:

Actively growing fungal discs of 7mm size in diameter were transferred to 100ml sterilized PDB medium. Different concentrations of α-$Al_2O_3$ were prepared according to the isolated fungal strain as follows: For A. flavus a concentration gradient of (0, 0.5, 1, 2 and 3 mg/100ml), while for Fusarium sp. (0, 0.5, 2, 4, 5 and 6mg/100ml) and Alternaria sp. (0, 5, 10, 20, 30 and 50 mg/100ml) to be suspended separately in the prepared PDB culture medium altogether with the fungal discs. The cultures were allowed to grow on shaker incubator 180rpm at 30$^oC$ for 5 days under ambient light condition. The fungal mycelia were harvested by filtration through desiccated, pre- weighted Whatman filter paper No.1 and dried overnight at 70$^oC$ then the fungal mycelial weights were recorded two following days till reach a constant volume.

## Results And Discussions

# 4.1. Structural Characterization

Figure 1 illustrates XRD of the preparation of α-$Al_2O_3$ using Pepsi cans. Figure 1 shows crystalline diffraction peaks at 2θ = 27.3°, 31.6°, 44.6°, 45.2°, 56.2°, 66.1° and 75.3° with cubic structure which agreed with JCPDS card 01-075-0278 which corresponded to Aluminum oxide (α-$Al_2O_3$).

The crystal size of both phases of Alumina is calculated using scherrerr equation [15]

$$D = 1ex\$0.915\lambda\$/-1ex\$\beta cos\theta\$ (1)$$

Where D is the crystal size, λ is the wavelength of X-ray, β (in radian) is the full width at half maximum (FWHM) of the diffraction peak and θ is the Bragg's diffraction angle (in degree) of the peak maximum. The average crystal size of α-$Al_2O_3$ is equal 38.8 nm. The crystallite size is belived to be the size of a coherently diffracting domain which isn't always the same as particle size [16].

The dislocation density, S, is a calculation of the extent of defects and vacancies in a crystal that can be calculated using the formula from the crystallite size (D) [17].

$$S = \frac{1}{D^2} (2)$$

S equal 6.64x$10^{-4}$ $nm^{-2}$ forα-$Al_2O_3$.

Figure 2 shows HRTEM image of α-Alumina using Pepsi cans. As seen in image the presence of a sponge-like mesoporous structure was detected with average particle size 4–10 nm.

Figure 3 represents FESEM for preparing α-Alumina using Pepsi cans. As shown in Fig. 3 this treatment, provide spongy structure with porous and homogenous aggregates with very small size. For EDX analysis as seen confirmed the presence of Al and Oxygen in addition to some element like Na and Cl which present in a small percentageeven after a good washing process, In spite of the washing process was so time-consuming.

Figure 4 represents ATR-FTIR of α-$Al_2O_3$. The bands at 3355 $cm^{-1}$ and 1629 $cm^{-1}$ for are corresponded to the stretching and bending vibration of O-H, respectively of adsorbed air. The bands at 872 $cm^{-1}$, 726 $cm^{-1}$, 532 $cm^{-1}$ and 477 $cm^{-1}$ are related to pseudo boehmite structure vibration for α Aluminum [18, 19].

# 4.2. Optical Properties

Figure 5 shows UV-Vis absorption spectra and optical band gap energy of α-$Al_2O_3$. The spectra shows strong absorption peaks at 245 nm for Aluminum oxide [20, 21]. This is due to electron photoexcitation from the valence band to the conduction band.

The direct optical band gap energy ($E_g$) of α-$Al_2O_3$ is calculated using Tauc relation [22]:

$(\alpha h\nu)^2 = \beta (h\nu - E_g)$ (3)

Where β is constant and α is the absorption coefficient and it is determined using the following relation [23]:

$$\alpha(\lambda) = \frac{2.303}{T} A (4)$$

Where A and T are the absorbance and the thickness of the prepared sample, respectively. Figure 7 (a and b) represent the plot of $(\alpha h\nu)^2$ against $h\nu$ of α-$Al_2O_3$. The direct optical band gap energy $E_g$ is calculated from the extrapolating the linear portion of the plot with photon energy ($h\nu$). As seen value of $E_g$ is 5.25 eV.

# 4.3. Fungal isolates characterization and identification

Among 15 fungal colonies obtained on rosebengal agar medium, 3 isolates were significantly different on morphological basis (colony shape, texture and medium pigmentation) Fig.6. Morphological and Microscopic examination of the mycelium and spores developed on PDA plates confirmed that the three isolates belonging to Aspergillus flavus, Fusarium oxysporum and Alternaria sp according to the taxonomy given by Ainsworth and James, 1971 [24] and Alexopoulos 1996 [25]. Our gathered data from the isolation and identification experimental method were compatible to the data obtained by Gulbis et al., 2016 [10] who confirmed that Fusarium, Alternaria and Aspergillus sp. were the most predominant fungal species in spoiled Maize and soybean grains. It's well known that Fusarium, Alternaria and Aspergillus sp. are the major Aflatoxin and Mycotoxin producing fungi in Maize, soy and small grain cereals reported by Gulbis et al., 2016 [10].

# 4.4. Screening of the antifungal activity

Figure 7 and Table 1 presents the effect of aluminum nanoparticles on the selected fungal strains growth inhibition in mm. all the fungal strains show variable sensitivity behavior against Al-nanoparticle. The [illegible] bitory activity was A. flavus followed by F. oxysporum with

inhibition zone 13.5 and 8 mm respectively. Alternaria sp. shows the less sensitivity action exposing to the selected nanoparticles with 1.5 mm inhibition zone

Table 1
Values of inhibition zone in mm on the selected fungal strains

| Strain ID | Inhibition zone (mm) |
|---|---|
| (A. Flavus) | 13.5 |
| (Alternaria Alternata) | 1.5 |
| (Fusarium oxysporum) | 8.0 |

# 4.5. Determination of the optimum fungicidal concentration against the fungal isolates.

Tables 2, 3 and 4 illustrates that the response of the fungal strain to gradient concentrations of Al-nanoparticles is different according to the fungal isolate.

Aspergillus flavus

Figure 8 exhibit that, the maximum inhibitory concentration detected for A. flavus was recorded in 1mg/100ml for with inhibition percentage (94.8 %) respectively.

Table 2
The response of the fungal strain to gradient concentrations of Al-nanoparticles for A. flavus.

| | Type A | |
|---|---|---|
| | DW | Inhibition % |
| 0 | 1.55 | |
| 0.5 | 0.17 | 89 |
| 1 | 0.08 | 94.8 |
| 2 | 0.08 | 94.8 |
| 3 | 0.08 | 94.8 |

Fusariumoxysporum

Data illustrated in Fig. 9 shows that, the maximum inhibitory concentration was detected for α-$Al_2O_3$ NPs percentage (98.6%).

Table 3
The response of the fungal strain to gradient concentrations of Al-nanoparticles for Fusarium oxysporum.

| | Type A | |
|---|---|---|
| | **DW** | **Inhibition %** |
| Control | **0.7** | |
| 0.5 | **0.09** | **87.14** |
| 2 | **0.08** | **88.57** |
| 4 | **0.06** | **91.43** |
| 5 | **0.05** | **92.86** |
| 6 | **0.01** | **98.57** |

The research data output is in correspondence to Suryavanshi et al., 2017 [26] study who evaluated the antifungal activity of aluminum nanoparticles against different food borne pathogenic fungi included fusarium oxysporum and Aspergillus flavus. The data showed that aluminum nanoparticles exhibited antifungal activity against F. oxysporum and A. flavus with MIC concentration of 250 and 150µg/ml respectively.

Moreover, Shenashen et al., 2016 [27] detected the antifungal activity of mesoporous aluminum nanoparticles against Fusarium Oxysporum and found that the highest antifungal activity was recorded at concentration 400mg/L with maximum inhibition percentage of 78.57% after growth on PDA plates in comparison to the control treatment.

Alternaria sp.

Figure 10 posed that, the highest growth inhibitory concentration was detected at 50mg/100ml value with inhibition percentage of 98.75%.

Table 4
The response of the fungal strain to gradient concentrations of Al-nanoparticles for Alternaria sp.

| | Type A | |
|---|---|---|
| | DW | Inhibition % |
| Control | 0.8 | |
| 5 | 0.2 | 75 |
| 10 | 0.13 | 83.75 |
| 20 | 0.07 | 91.25 |
| 30 | 0.01 | 98.75 |
| 50 | 0.01 | 98.75 |

The fungicidal effect of aluminum nanoparticles may be explained by multiple cellular site destruction: either due to its direct linkage to protein and enzymes molecules or DNA contact which causes mutation and adversely affect cellular replication. The antifungal activity may also attribute to linkage to the free hydrogen bond on the cellular membrane which alter the lipopolysaccharide layer configurations that eventually lead to cell membrane damage and cell lysis reported by Capeletti et al., 2014 [28].

## Conclusion

The structural, morphological, optical and fungicidal activity of α-$Al_2O_3$ are studied. XRD, FESEM, EDX and ATR –FTIR confirmed the formation of $Al_2O_3$. The average crystal size and dislocation density of α-$Al_2O_3$ are found to be 38.8 nm and $6.64x10^{-4}$ $nm^{-2}$. HRTEM shows the average particle size of α-$Al_2O_3$ is 4–10 nm. FESEM of α-$Al_2O_3$ has spongy structure with porous and homogenous aggregates. UV-Vis spectra of α-$Al_2O_3$ has strong peaks at 245 nm. The antifungal activity of α-$Al_2O_3$ against A. flavus, Fusarium sp. and Alternaria sp. show maximum antifungal activity at concentrations 1, 6 and 50 mg/100ml, respectively.

## Declarations

# Acknowledgment

This study was financially supported by National Research Centre of Egypt through internal research project no. 12020216.

## References

1. M. Premanathan, K. Karthikeyan, K. Jeyasubramanian, G. Manivannan, Selective toxicity of ZnO nanoparticles toward Gram-positive bacteria and cancer cells by apoptosis through lipid peroxidation. Nanomed. Nanotechnol. Biol. Med. **7**(2), 184–192 (2011)
2. N. Beyth, Y. Houri-Haddad, A. Domb, W. Khan, R. Hazan (2015). Alternative antimicrobial approach: nano-antimicrobial materials. Evidence-based complementary and alternative medicine, 2015
3. T.K. Sheel, P. Poddar, A.B.M.W. Murad, A.J. Neger, M. T., A.M.S. Chowdhury (2016). Preparation of aluminum oxide from industrial waste can available in Bangladesh environment: SEM and EDX analysis. Journal of Advanced Chemical Engineering, 6(2)
4. R. Galindo, I. Padilla, O. Rodríguez, R. Sánchez-Hernández, S. López-Andrés, A. López-Delgado (2015). Characterization of solid wastes from aluminum tertiary sector: the current state of Spanish industry
5. S.M. Kaufmann, N. Goldstein, K. Millrath, N.J. Themelis, *State of Garbage in America–14th Annual Nationwide Survey of Solid Waste Management in the United States* (NY, USA, 2004)
6. Z. Zhang, T.J. Pinnavaia, Mesostructured Forms of the Transition Phases η-and χ-Al2O3. Angew. Chem. Int. Ed. **47**(39), 7501–7504 (2008)
7. K.A. Matori, L.C. Wah, M. Hashim, I. Ismail, M.H.M. Zaid, Phase transformations of α-alumina made from waste aluminum via a precipitation technique. Int. J. Mol. Sci. **13**(12), 16812–16821 (2012)
8. W.L. Suchanek, Hydrothermal synthesis of alpha alumina (α-Al2O3) powders: study of the processing variables and growth mechanisms. J. Am. Ceram. Soc. **93**(2), 399–412 (2010)
9. J. Pleadin, Mycotoxins in grains and feed: Contamination and toxic effect in animals. Biotechnology in Animal Husbandry **31**(4), 441–456 (2015)
10. K. Gulbis, B. Bankina, G. Bimšteina, I. Neusa-Luca, A. Roga, D. Fridmanis, fungal diversity of maize (zea mays l.). Grains. Rural sustainability research **35**, 330 (2016)
11. C.A.L. Abe, C.B. Faria, F.F. De Castro, S.R. De Souza, F.C.D. Santos, C.N. Da Silva, D. Tessmann, I.P. Barbosa-Tessmann, Fungi isolated from maize (Zea mays L.) grains and production of associated enzyme activities. Int. J. Mol. Sci. **16**(7), 15328–15346 (2015)
12. A. Derbalah, M. Shenashen, A. Hamza, A. Mohamed, E. Safty, S, Antifungal activity of fabricated mesoporous silica nanoparticles against early blight of tomato. Egyptian journal of basic and applied sciences **5**(2), 145–150 (2018)
13. J. Weiss, P. Takhistov, D.J. McClements, Functional materials in food nanotechnology. Journal of food science **71**(9), R107 (2006)
14. R. Nair, S.H. Varghese, B.G. Nair, T. Maekawa, Y. Yoshida, D.S. Kumar, Nanoparticulate material delivery to plants. Plant science **179**(3), 154–163 (2010)
15. A. Patterson, The Scherrer Formula for X-Ray Particle Size Determination. Phys. Rev. **56**(10), 978–982 (1939)
16. P. Bindu, S. Thomas, Estimation of lattice strain in ZnO nanoparticles: X-ray peak profile analysis. Journal of Theoretical and Applied Physics **8**(4), 123–134 (2014)

17. M.J. Chithra, M. Sathya, K. Pushpanathan, Effect of pH on crystal size and photoluminescence property of ZnO nanoparticles prepared by chemical precipitation method. Acta Metall. Sin. **28**(3), 394–404 (2015)
18. C. Liu, K. Shih, Y. Gao, F. Li, L. Wei, Dechlorinating transformation of propachlor through nucleophilic substitution by dithionite on the surface of alumina. J. Soils Sediments **12**(5), 724–733 (2012)
19. G. Zu, J. Shen, X. Wei, X. Ni, Z. Zhang, J. Wang, G. Liu, Preparation and characterization of monolithic alumina aerogels. J. Non-cryst. Solids **357**(15), 2903–2906 (2011)
20. P.A. Prashanth, R.S. Raveendra, H. Krishna, R. Ananda, S. Bhagya, N.P. Nagabhushana, B.M. Lingaraju, K. Raja, H. Naika, Synthesis, characterizations, antibacterial and photoluminescence studies of solution combustion-derived α-Al2O3 nanoparticles. J. Asian. Ceam. Soc. **3**(3), 345–351 (2015)
21. X. Yuan, J. Zhu, K. Tang, Y. Cheng, Z. Xu, W. Yang, Formation and properties of 1-D alumina nanostructures prepared via a template-free thermal reaction. Procedia engineering **102**, 602–609 (2015)
22. J. Tauc (1966). The optical properties of solids
23. T. Siddaiah, P. Ojha, N.O. Kumar, C. Ramu (2018). Structural, optical and thermal characterizations of PVA/MAA: EA polyblend films. Materials Research, 21(5)
24. G.C. Ainsworth (1971). Ainsworth and Bishys Dictionary of fungi:(P. 412) Commonwealth Mycological Institute. Kew, Surry, England
25. C.J. Alexopoulos, C.W. Mims, M. Blackwell, *Introductory mycology (No. Ed. 4)* (John Wiley and Sons, 1996)
26. P. Suryavanshi, R. Pandit, A. Gade, M. Derita, S. Zachino, M. Rai, Colletotrichum sp.-mediated synthesis of sulphur and aluminium oxide nanoparticles and its in vitro activity against selected food-borne pathogens. LWT-Food Science and Technology **81**, 188–194 (2017)
27. M. Shenashen, A. Derbalah, A. Hamza, A. Mohamed, E. Safty, S, Antifungal activity of fabricated mesoporous alumina nanoparticles against root rot disease of tomato caused by Fusarium oxysporium. Pest management science **73**(6), 1121–1126 (2017)
28. L.B. Capeletti, L.F. de Oliveira, K.D.A. Goncalves, J.F.A. de Oliveira, A. Saito, J. Kobarg, J. Santos, M.B. Cardoso, Tailored silica–antibiotic nanoparticles: overcoming bacterial resistance with low cytotoxicity. Langmuir **30**(25), 7456–7464 (2014)

# Figures

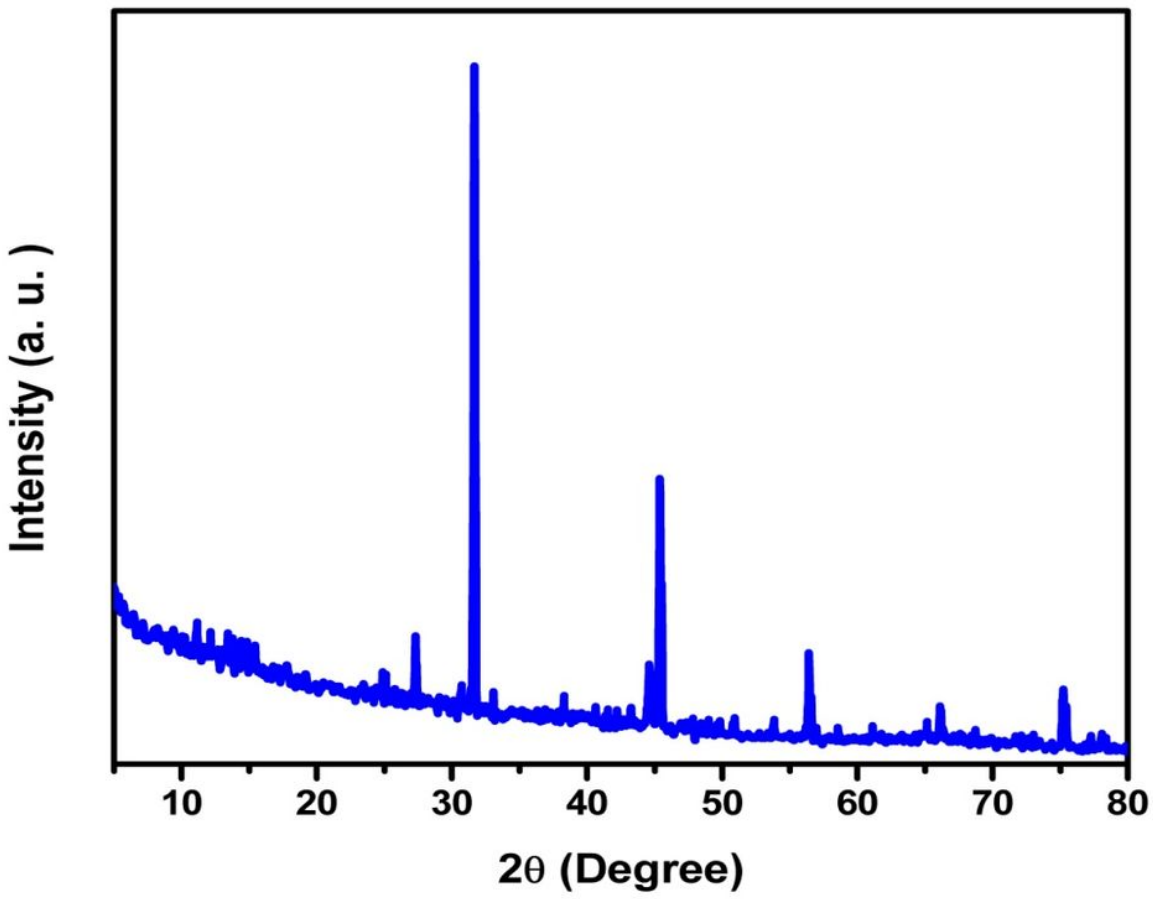


**Figure 1**

XRD patterns of α-Al2O3

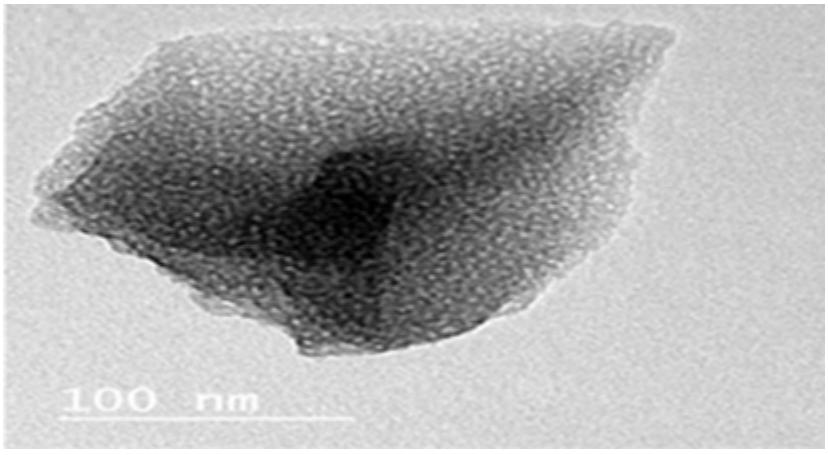


**Figure 2**

HRTEM of α-Al2O3

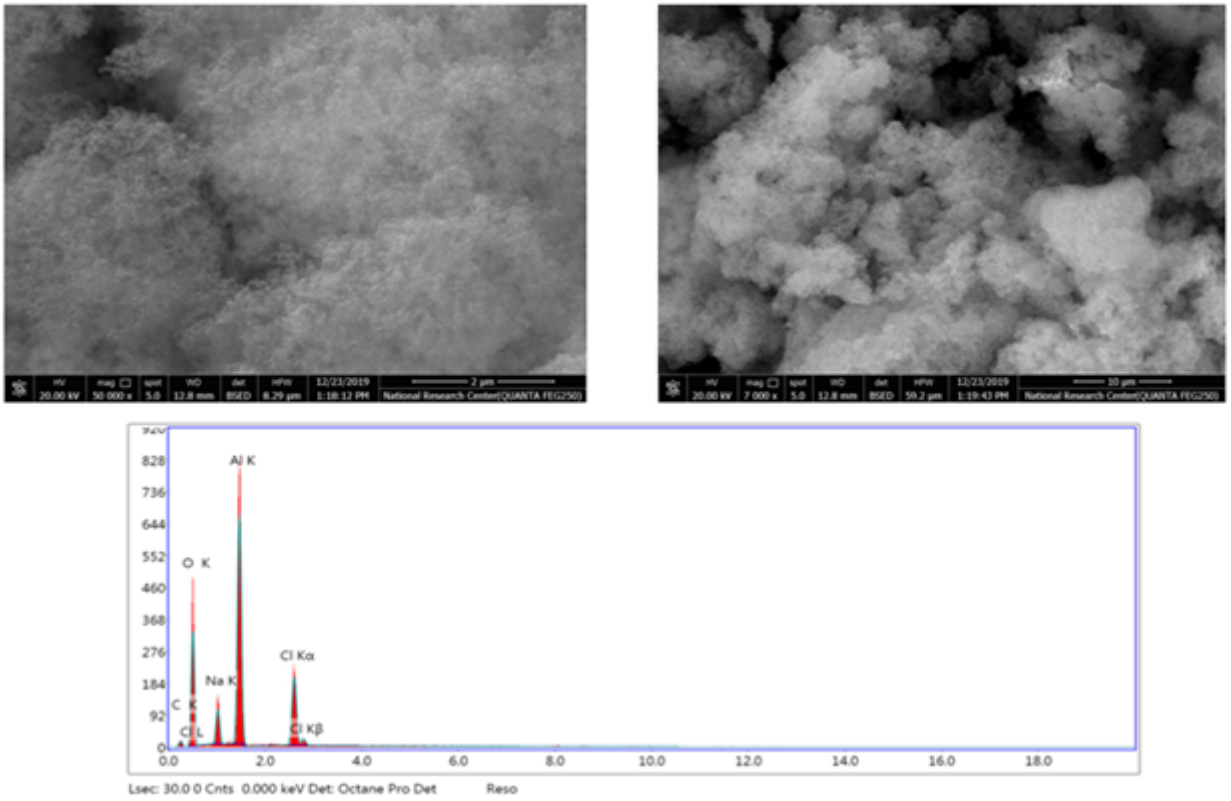


**Figure 3**

FESEM and EDX of α-Al2O3

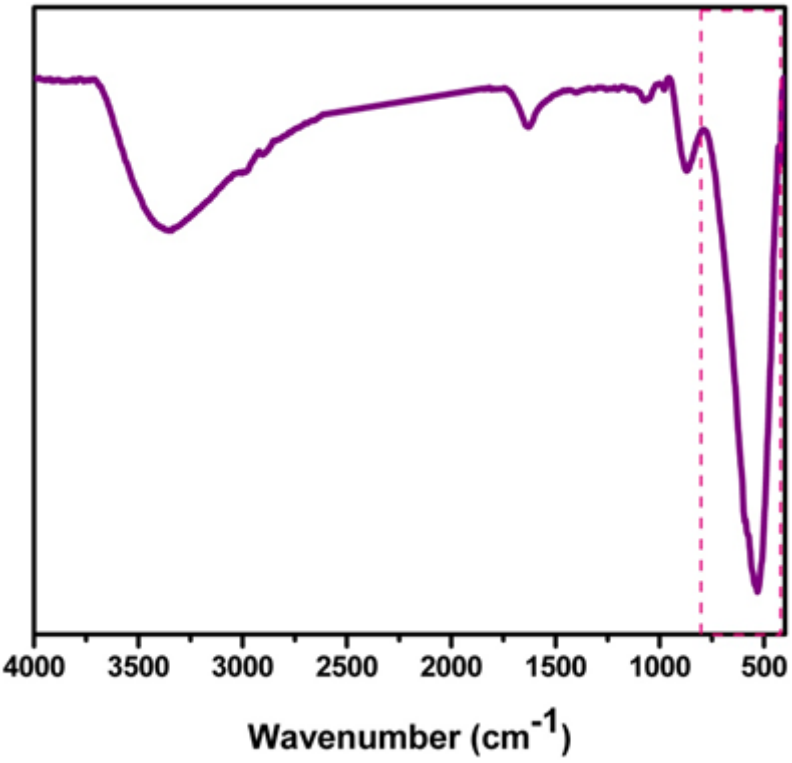


**Figure 4**

Loading [MathJax]/jax/output/CommonHTML/jax.js α-Al2O3

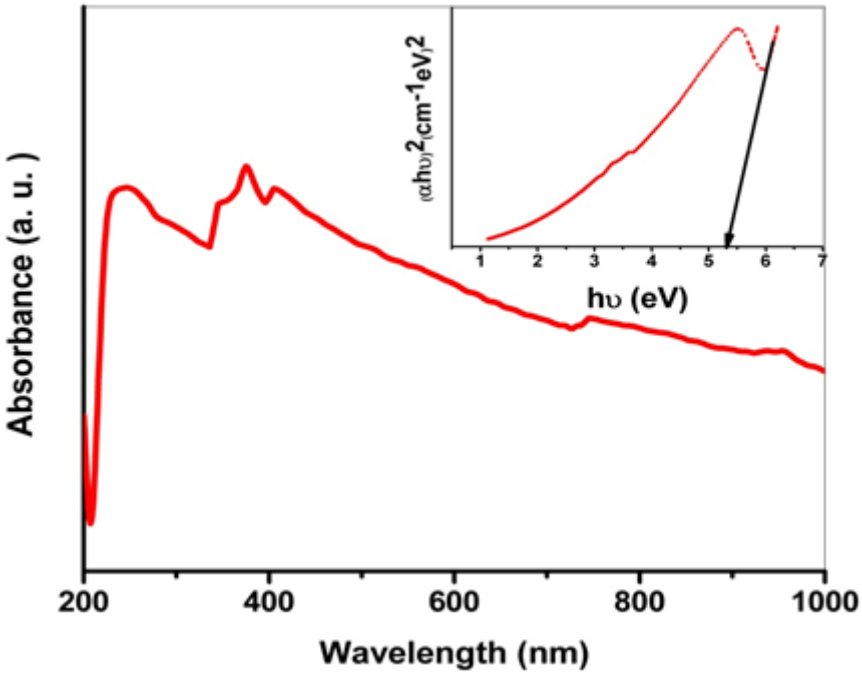


## Figure 5

UV-Vis and Direct optical band gap spectra of α-Al2O3

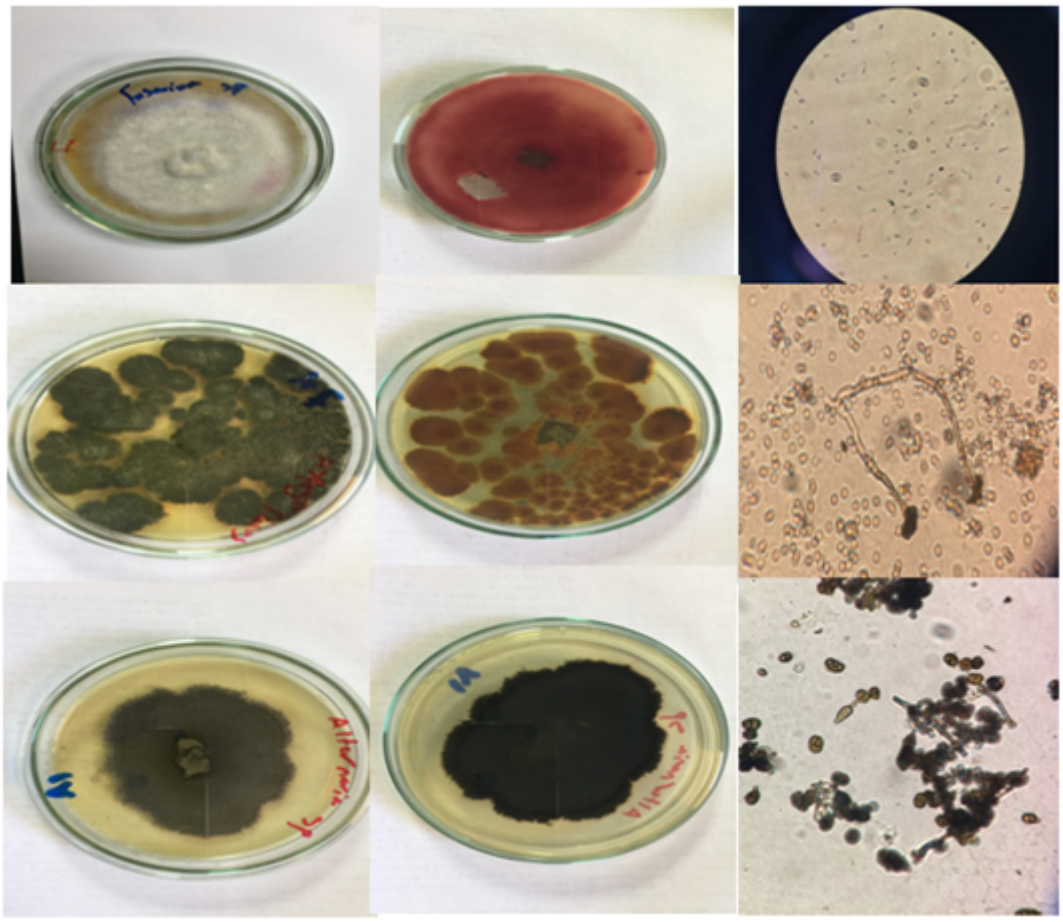

## Figure 6

Morphological and microscopical characteristics of fungal isolates obtained from maize and soy grains.

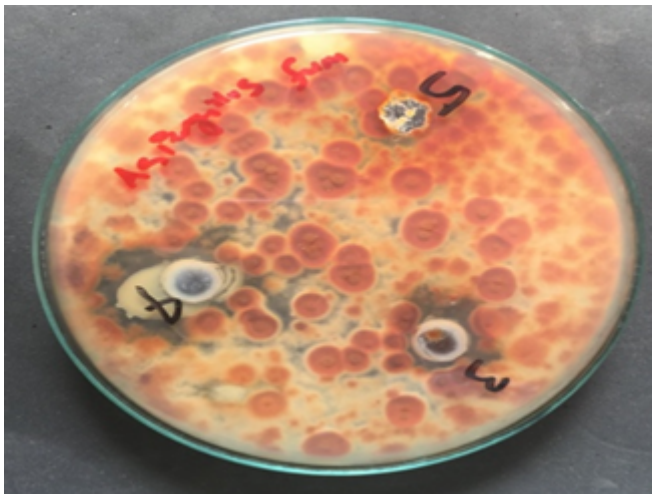

**Figure 7**

the effect of α-Al2O3 NPs on the selected fungal strains.

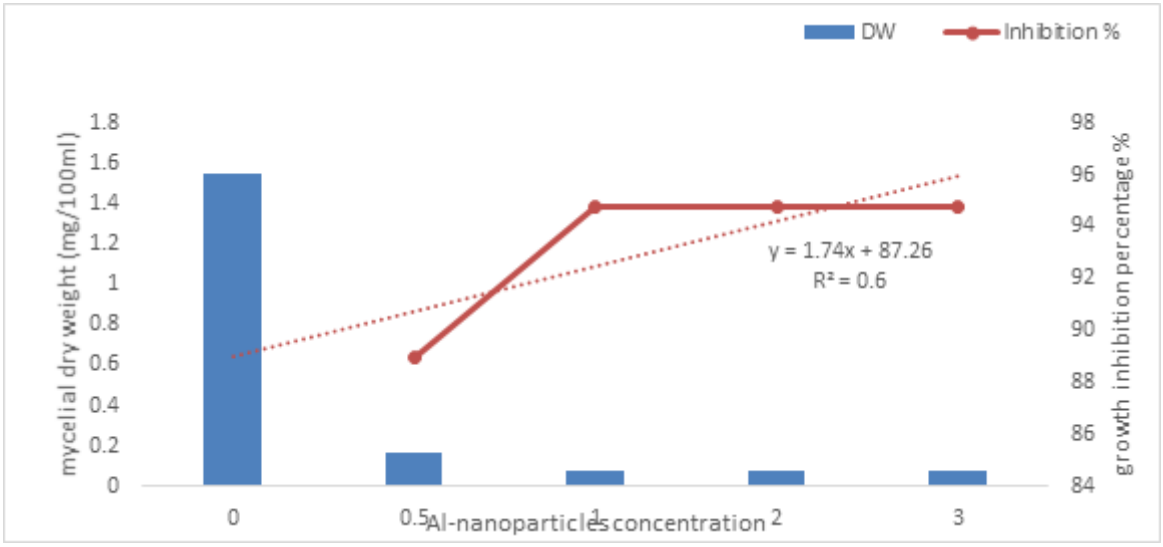


**Figure 8**

shows the optimum fungicidal concentration for α-Al2O3 NPs against A. flavus.

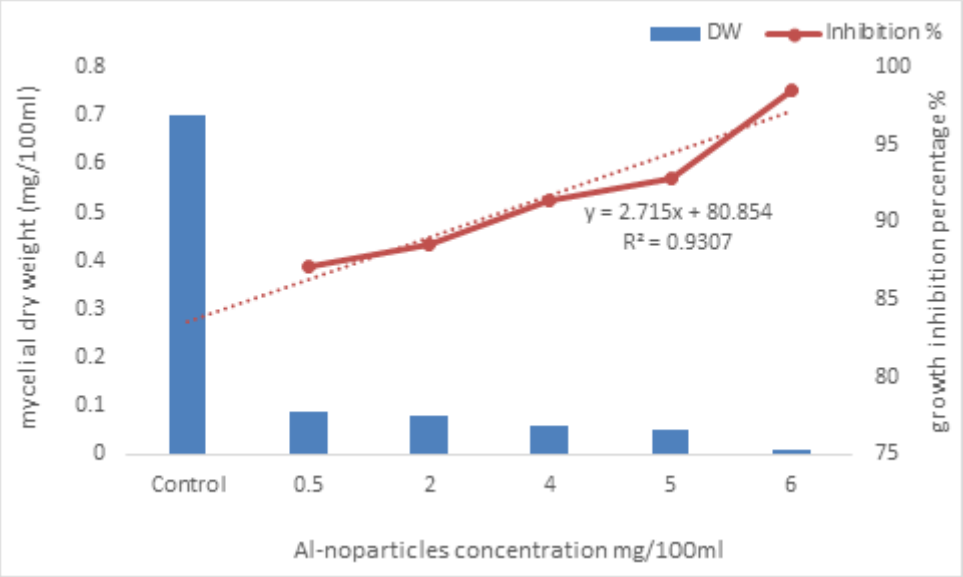


**Figure 9**

shows the optimum fungicidal concentration for α-Al2O3 NPs against Fusarium oxysporum.

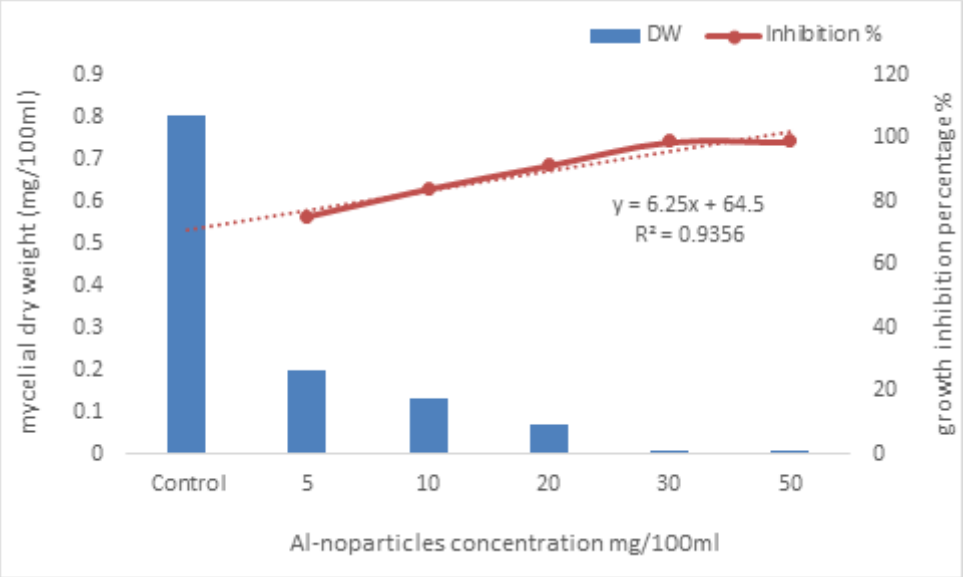


**Figure 10**

shows the optimum fungicidal concentration for α-Al2O3 NPs against Alternaria sp.